HHS Public Access

Author manuscript

Antiviral Res. Author manuscript; available in PMC 2016 November 08.

Published in final edited form as:

Antiviral Res. 2014 June ; 106: 53–60. doi:10.1016/j.antiviral.2014.03.011.

Evaluation of luciferase and GFP-expressing Nipah viruses for rapid quantitative antiviral screening

Michael K. Lo[*], **Stuart T. Nichol**, and **Christina F. Spiropoulou**[*]

Viral Special Pathogens Branch, Centers for Disease Control and Prevention, Atlanta, GA, United States

Abstract

Nipah virus (NiV) outbreaks have occurred in Malaysia, India, and Bangladesh, and the virus continues to cause annual outbreaks of fatal human encephalitis in Bangladesh due to spillover from its bat host reservoir. Due to its high pathogenicity, its potential use for bio/agro-terrorism, and to the current lack of approved therapeutics, NiV is designated as an overlap select agent requiring biosafety level-4 containment. Although the development of therapeutic monoclonal antibodies and soluble protein subunit vaccines have shown great promise, the paucity of effective antiviral drugs against NiV merits further exploration of compound libraries using rapid quantitative antiviral assays. As a proof-of-concept study, we evaluated the use of fluorescent and luminescent reporter NiVs for antiviral screening. We constructed and rescued NiVs expressing either Renilla luciferase or green fluorescent protein, and characterized their reporter signal kinetics in different cell types as well as in the presence of several inhibitors. The 50% effective concentrations (EC_{50}s) derived for inhibitors against both reporter viruses are within range of EC_{50}s derived from virus yield-based dose–response assays against wild-type NiV (within $1Log_{10}$), thus demonstrating that both reporter NiVs can serve as robust antiviral screening tools. Utilizing these live NiV-based reporter assays requires modest instrumentation, and circumvents the time and labor-intensive steps associated with cytopathic effect or viral antigen-based assays. These reporter NiVs will not only facilitate antiviral screening, but also the study of host cell components that influence the virus life cycle.

Keywords

Henipavirus; Nipah virus; Antiviral screening; Luciferase; GFP; High-throughput screening

1. Introduction

Nipah virus (NiV) is a highly pathogenic paramyxovirus in the genus *Henipavirus* of the subfamily *Paramyxovirinae* within the family *Paramyxoviridae* (Rota and Lo, 2012). Humans are infected upon spillover of NiV from its bat reservoir host or by person-to-person transmission (Luby, 2013). Due to its high pathogenicity, its potential use for bio/

[*]Corresponding authors. Address: Centers for Disease Control and Prevention, Viral Special Pathogens Branch, 1600 Clifton Road, Mailstop G-14, Atlanta, GA 30333, United States. Tel.:+1 4046390327 (M.K. Lo). mko2@cdc.gov (M.K. Lo), ccs8@cdc.gov (C.F. Spiropoulou).

agro-terrorism, and to the current lack of approved therapeutics, NiV is designated as an overlap select agent requiring biosafety level-4 containment. Although several preventative measures against exposure to bat saliva or urine have been studied (Nahar et al., 2013), NiV continues to cause near-annual outbreaks of fatal encephalitis in Bangladesh. The development of therapeutic monoclonal antibodies and soluble subunit vaccines against henipaviruses have shown great promise (Broder et al., 2013), but screening available compound libraries for potentially efficacious therapeutics against NiV remains a high priority for investigation. Most high-throughput antiviral assays against NiV were developed to screen for inhibitors of virus entry and/or cell-to-cell fusion (Bossart et al., 2005; Porotto et al., 2009; Talekar et al., 2012; Tamin et al., 2009), while the NiV minigenome assay was used to screen for inhibitors of NiV replication (Freiberg et al., 2008). A chemiluminescent immunodetection assay for live henipavirus infection significantly streamlined antiviral screening when compared with cytopathic effect (CPE) or immune plaque-based assays, but had relatively limited signal-to-noise ratios (<100), and also required cell fixation and multiple incubation steps which are time and labor-intensive (Aljofan et al., 2008). Reverse genetic systems for henipaviruses have enabled the generation of recombinant viruses expressing fluorescent or luminescent proteins which allow for rapid detection of infection *in vitro* and *in vivo* (Lo et al., 2012; Marsh et al., 2013; Yoneda et al., 2006). We sought to determine whether NiVs expressing fluorescent or luminescent reporters could facilitate rapid quantitative antiviral screening. As a proof-of-concept study, we constructed and rescued NiVs expressing either Renilla luciferase (LUC2AM) or green fluorescent protein (GFP2AM), characterized their reporter signal kinetics in different human cell types, and tested them in parallel against cellular inhibitors of pyrimidine biosynthesis as well as innate immune agonists. We show that both reporter viruses can be used in the 96-well format and have excellent signal-to-noise ratios and Z'-factors. Furthermore, the 50% effective concentrations (EC_{50}s) derived for inhibitors tested against both reporter viruses were not only within close range of one another (within 4-fold), but also of EC_{50}s derived from virus yield-based dose–response assays against wild-type NiV (within 1 Log_{10}), thus demonstrating that both reporter NiVs can serve as robust antiviral screening tools.

2. Materials and methods

2.1. Cells

Vero (African green monkey kidney), A549 (human lung epithelial carcinoma), HeLa (human cervical carcinoma), and HEK 293T (human embryonic kidney) cells were maintained at 37 °C and 5% CO_2 in Dulbecco's modified Eagle's medium supplemented with 7.5% fetal bovine serum (FBS), 100 U/mL penicillin, 100 μg/mL streptomycin, and 2 mM L-glutamine. Baby hamster kidney cells stably expressing T7 polymerase (BSRT7/5) (Buchholz et al., 1999) were incubated at every third passage in the presence of 1 mg/mL G-418 (Geneticin).

2.2. Cloning and rescue of recombinant viruses

For LUC2AM, a modified NiV M gene fragment expressing the Renilla luciferase (Promega) open reading frame (ORF) in-frame with the NiV Matrix (M) gene ORF separated by the FMDV 2A protease cleavage peptide was constructed using a 4-step

overlapping PCR strategy as described for a DsRed-Express reporter NiV (RED2AM) and inserted into a plasmid containing a full-length cDNA copy of wild-type recombinant NiV genome using engineered SbfI and SacII restriction sites (Lo et al., 2012). The total genome length of LUC2AM was 19,254 nt.

The GFP2AM expressing the green fluorescence protein Zsgreen1 (Clontech) ORF in-frame with the NiV M gene ORF separated by the porcine teschovirus 2A (p2A) protease cleavage peptide was constructed using a second-generation wild-type recombinant NiV (rNiV) (Genbank sequence AF212302) devoid of engineered restriction sites, assembled via 4 fragments into the same plasmid backbone used for LUC2AM (Genscript). A synthesized fragment containing the GFP, p2A, and NiV M coding sequence in-frame was cloned into WT using PacI restriction sites. An additional 3 nucleotides "GGA" encoding the amino acid glycine were inserted between the end of the Zsgreen1 ORF and the start of the p2A cleavage peptide for the final genome length to obey the "Rule of six" at 19,014 nt (Kolakofsky et al., 1998). Both LUC2AM and GFP2AM were rescued as previously described (Lo et al., 2012). The genomes of the rescued viruses were fully sequenced with no undesired mutations. Virus stock titers were determined by median tissue culture infectious dose ($TCID_{50}$) assay (see below).

2.3. Infections with recombinant reporter viruses, reporter activity measurements, cell type optimization, $TCID_{50}$

All infections in this study were performed in 96-well plates. Cells were seeded in opaque black or white plates (Costar 3916, 3917) for fluorescence and luminescence-based assays respectively. Initial time course experiments for rescued viruses were performed by infecting 2×10^4 Vero cells/well at multiplicity of infection (MOI) = 0.01 $TCID_{50}$/cell of either virus for 2 h. Virus inoculum was removed and replaced with 100 μL Fluorobrite medium (Life Technologies) supplemented with 2 mM L-glutamine and 10% FBS. At 24, 48, and 72 h post-infection (hpi), supernatants were harvested for $TCID_{50}$ determination and replaced with Fluorobrite medium. Fluorescence activity (gain = 65) was measured in a H1 Synergy plate reader (Biotek), while luminescence activity (gain = 107) was measured in the same reader 10 min after addition of Renilla-Glo substrate (Promega). Subsequent infections were performed at MOI = 0.2 $TCID_{50}$/cell unless stated otherwise. Cytopathic effect-based $TCID_{50}$ assays were performed by infecting Vero cells in 10-fold dilution series of samples (10^{-1}–10^{-8}) in a 96- well plate format, infecting 9 wells per sample and dilution step. Plates were read after 7 days to ensure a clear distinction between infected and uninfected wells at the highest dilutions.

2.4. Fluorescence microscopy

2×10^4 HeLa cells were infected with LUC2AM or GFP2AM, and at 24 hpi were fixed in 10% formalin for 15 min, permeablized with PBS + 0.4% Triton-X for 5 min, washed with PBS + 0.1% Tween (PBS-T), and blocked with PBS-T + 5% milk (PBS-T-M) for 30 min. LUC2AM-infected cells were incubated with a mouse anti-NiV-N monoclonal antibody 1A11C1 (Chiang et al., 2010) and a rabbit anti-Renilla luciferase antibody (MBL) diluted 1:1000 and 1:200 respectively in PBS-T-M for 1 h at 37 °C, while GFP2AM-infected cells were incubated with only 1A11C1 antibody. After 3 washes with PBS-T, cells were

incubated with anti-mouse DyLight 550 and anti-rabbit DyLight 488 antibodies (Bethyl Laboratories, Inc.) diluted 1:1000 in PBS-T-M for 30 min at 37 °C. After 3 washes, fluorescence images were taken on a Zeiss Axiovert 200 microscope at 40X magnification.

2.5. Antiviral compounds, assessment of cell viability (CC_{50}) and 50% effective concentrations (EC_{50})

The following compounds used in this study were dissolved in dimethyl sulfoxide (DMSO): 6-azauridine acetate (Sigma), Pyrazofurin (TRC), and compound 09167 (Vitas-M Laboratory) (Yan et al., 2013). The final DMSO concentration in Fluorobrite media was 0.1%. Universal interferon (U-IFN) (Sigma) was dissolved in sterile distilled H_2O. The CellTiter-Glo assay (Promega) was used to determine viability of uninfected 293T cells exposed to 3-fold serial dilutions of the compounds for 48 h. Values were normalized to DMSO controls according to % viability as follows: % viability = [(specific value–reference value)/(DMSO control value − reference value)] × 100. Reference values were derived from control wells without cells. DMSO control values (after subtraction of reference values) were set at 100% viability. 50% viability/cytotoxicity (CC_{50}) and 50% effective concentrations (EC_{50}) were calculated using four-parameter variable slope non-linear regression fitting of mean values for three experiments. Therapeutic indices (TI) were represented as CC_{50}/EC_{50}. In instances which CC_{50} could not be properly calculated due to non-convergence of dose response curves, we designated the highest concentration of compound used as the CC_{50}.

2.6. Statistical analysis

Statistical analysis was performed using Prism 6 software (GraphPad Software). Z' (separation band/dynamic range of the assay) values were calculated based on the following formula: $Z' = 1 - [(3SD_C + 3SD_B)/(mean_C - mean_B)]$, where SD is the standard deviation, C is the control, and B is the background (Zhang et al., 1999). The percent coefficient of variation (%CV) was calculated as follows: $\%CV = SD_C/mean_C \times 100$.

3. Results and discussion

3.1. Construction and characterization of luciferase and GFP expressing NiVs

To evaluate the use of luminescent reporters for antiviral screening against NiV, we constructed a Renilla luciferase-expressing NiV (LUC2AM) by employing previous methods used to generate a red fluorescent protein-expressing NiV (RED2AM) (Lo et al., 2012). We inserted the Renilla luciferase (LUC) gene into the NiV matrix (M) gene 5′ of the MORF in the same reading frame, separated by the coding sequence of the Foot and Mouth Disease virus protease cleavage peptide (F2A) (Fig. 1A). We used the same strategy to construct a second generation recombinant green fluorescent protein(GFP)-expressing NiV (GFP2AM), except that we used the more efficiently-cleaved porcine Teschovirus 2A cleavage peptide (p2A) coding sequence instead of F2A (Kim et al., 2011) (see Section 2). We rescued both LUC2AM and GFP2AM and confirmed expression of their respective reporter proteins by immunofluorescence microscopy. The distribution of both LUC and GFP were distinct from NiV nucleoprotein, with the luciferase localizing exclusively to the cytoplasm, and with the GFP occupying both nuclear and cytoplasmic compartments (Fig.

1B). While GFP2AM grew similarly in Vero cells (MOI = 0.01 $TCID_{50}$/cell) compared with the non-reporter recombinant (rNiV) (Fig. 1C, right) LUC2AM had an attenuated growth phenotype when compared with its corresponding first generation non-reporter recombinant NiV (WT) (Fig. 1C, left). This is consistent with previous observations that the RED2AM virus was moderately attenuated compared with WT (Lo et al., 2012). Furthermore our result is consistent with previous work showing that NiV M requires ubiquitination inside the nucleus to become functional for budding (Wang et al., 2010), since the comparatively less-efficient cleavage of F2A would result in decreased amounts of functional NiV M for budding new virus particles. In spite of this phenotype however, LUC2AM generated increasing levels of LUC activity from 0 to 48 h postinfection (hpi), and reached viral titers of over 10^6 $TCID_{50}$/mL by 72 hpi (Fig. 1C, left panel). The fluorescence signal generated by GFP2AM was detectable at 24 hpi, but increased by greater than 20-fold at 48 hpi, and continued to increase through 72 hpi. The accumulation of GFP signal over the course of infection corresponded with the increase in GFP2AM viral titer (Fig. 1C, right panel).

3.2. Optimization of cell type and infection conditions for LUC2AM and GFP2AM-based assays

We then optimized both assays for antiviral testing. We tested each virus against 3 common human cell lines (A549, HeLa, 293T) alongside Vero cells to determine which would yield the strongest reporter signal over the course of infection. For negative controls, we assayed for reporter activity in each cell line infected with wild-type recombinant NiV (rNiV). Infection with LUC2AM over the course of 72 h (MOI = 0.1 $TCID_{50}$/cell) showed that HeLa and 293T cells supported peak LUC activity to approximately equal or greater levels than in Vero cells, while A549 only marginally supported LUC activity (Fig. 2A, left panel). In both Vero and HeLa cells, LUC signal peaked at 24 hpi (~4–5 × 10^4 relative light units) and steadily decreased by over 10-fold by 72 hpi. In 293T cells however, the LUC signal was approximately equal to those of Vero and HeLa cells at 24 hpi, but proceeded to double by 48 hpi (~8 × 10^4 RLU) before decreasing at 72 hpi to levels similar to 24 hpi. Infection with GFP2AM yielded similar results, showing minimal NiV replication in A549 cells, and indicating 293T cells as the optimal cell type which generated the highest GFP signal onward from 48 hpi to 72 hpi (Fig. 2A right panel). In contrast to the LUC2AM infections however, all 4 infected cell lines attained their highest levels of GFP expression at 72 hpi. The different reporter signal kinetics observed when comparing LUC2AM and GFP2AM infections are likely a function of respective reporter protein maturation rates and half-lives. Whereas LUC matures rapidly and has a protein half-life of approximately 14 h in the cell cytoplasm (Loening et al., 2006), GFP requires 8–12 h for maturation, and has a protein half-life of approximately 26 h (Corish and Tyler-Smith, 1999). Since the peak LUC signal in infected 293T cells occurred at 48 hpi, and because of the minimal difference in GFP signal between 48 hpi and 72 hpi, we chose 48 hpi as our assay time point for both LUC2AM and GFP2AM.

To further optimize these reporter assays, we infected 293T cells with either reporter virus at MOIs ranging from 0.05 to 0.4 $TCID^{50}$/cell. Increasing the MOI for both LUC2AM and GFP2AM led to corresponding increases in reporter activity (Fig. 2B). Since the increase in MOI from 0.2 to 0.4 for both LUC2AM and GFP2AM only marginally increased their

respective reporter activity (less than 2-fold), we used MOI = 0.2 $TCID_{50}$/cell for both reporter viruses for our antiviral assays. We performed growth curves for both viruses in 293T cells by infecting at MOI = 0.2 $TCID_{50}$/cell, and observed increases in reporter signals corresponding with increases in virus titers (Fig. 2C).

3.3. Testing antiviral inhibitors against LUC2AM and GFP2AM

Having optimized both fluorescent and luminescent reporter assays in 293T cells, we assayed LUC2AM and GFP2AM against two known inhibitors of NiV, 6-azauridine acetate and pyrazofurin. Both of these compounds inhibit cellular pyrimidine biosynthesis via blocking orotidine 5′-monophosphate decarboxylase (Bono et al., 1964; Georges-Courbot et al., 2006; Gutowski et al., 1975). Consistent with a prior study utilizing a CPE-based assay (Georges-Courbot et al., 2006), 6-azauridine acetate and pyrazofurin showed dose-dependent inhibition of LUC2AM and GFP2AM, reducing reporter activity to background levels at the highest doses (25–50 μM) while having mild to minimal effects on cell viability (Fig. 3A). The respective 50% effective concentrations (EC_{50}) determined for each compound using the LUC2AM and GFP2AM were within 3-fold of each other (Table 1).

Since several studies have demonstrated the sensitivity of henipaviruses to type-1 interferon (IFN) signaling (Dhondt et al., 2013; Escaffre et al., 2013; Virtue et al., 2011), we evaluated the antiviral effect of universal interferon (U-IFN) against our reporter viruses. Although increasing concentrations of U-IFN led to corresponding decreases in respective reporter activity, even the highest concentration (1000 IU) of U-IFN only reduced LUC and GFP activity by approximately 4-fold and 3-fold respectively (Fig. 3B, top panels). These results are consistent with the early expression of multiple antagonists of IFN signaling by NiV (Kulkarni et al., 2009; Rodriguez et al., 2002; Shaw et al., 2005). EC_{50} values for U-IFN against LUC2AM and GFP2AM were nearly identical (Table 1). In addition to U-IFN we also tested compound 09167, a recently characterized agonist of the innate antiviral response (Yan et al., 2013) (Fig. 3B, lower panels). In contrast to U-IFN, treatment with compound 09167 was able to completely ablate both LUC and GFP activity at the highest dose tested (12.5 μM), indicating that IFN signaling-independent components have crucial roles in blocking NiV replication. Dose response curves for compound 09167 against both LUC2AM and GFP2AM confirmed sub-micro molar EC_{50}s, which were consistent with EC_{50}s previously obtained for 09167 against other paramyxoviruses (Yan et al., 2013) (Table 1). Further studies of this compound's effect on cell viability are warranted to determine its suitability for antiviral testing *in vivo*.

3.4. Counter screening against wild-type NiV, evaluating reporter assays for high-throughput screening

To confirm whether the dose–response curves and EC_{50} values obtained using these reporter viruses reflected actual inhibition of NiV replication, we tested 6-azauridine acetate and compound 09167 against wild-type non-recombinant NiV via virus yield-based dose–response assays (Fig. 4A). We observed dose-dependent reductions in virus titers to below initial levels of input virus at the two highest doses for each compound (>4 Log_{10} $TCID_{50}$/mL reduction), suggesting complete ablation of viral replication at these concentrations. EC_{50} values calculated for 6-azauridine and 09167 against wild-type NiV

were within 1 Log_{10} of EC_{50} values derived for each compound against LUC2AM and GFP2AM, indicating that inhibition of the reporter viruses paralleled inhibition of NiV replication (Fig. 4B, Table 1). The moderately higher EC_{50}s calculated from the reporter viruses suggest a lesser likelihood to detect false positives in the context of high-throughput screening (HTS). To quantitatively assess the suitability of these two viruses for HTS, we used compound 09167 as a positive control for inhibition and calculated Z' factor values, signal-to-noise ratios, and coefficients of variation for the 96-well plate format used throughout this study. For both assays, these values were robust and well within the acceptable range for HTS (Zhang et al., 1999) (Table 2).

4. Conclusions

The primary advantages to using viral reporter assays over viral antigen-based assays are the significant reduction in assay turnaround time and the minimal reagents required. Whereas a previously described henipavirus immunodetection assay required at least 2 h of post-infection processing (fixing, blocking, antibody staining) before the plate reading step, the LUC2AM assay required just 10 min of reagent incubation before plate reading, while the GFP2AM assay required even less time since no additional reagents were required. The LUC2AM assay has several advantages over the GFP2AM assay including better signal-to-noise ratios and less variability between samples/wells. Although we established the LUC2AM assay to be read alongside the GFP2AM assay at 48 hpi, the robust signal-to-noise ratio and Z' values for LUC2AM at even 24 hpi would allow for adaptation of the assay to span a shorter infection period, whereas this would not be possible for GFP2AM due to its longer maturation time (data not shown). The GFP2AM assay has some advantages over LUC2AM assay in that GFP activity can be measured multiple times, whereas LUC measurement is an endpoint measurement. Furthermore, GFP2AM can be easily adapted for high content imaging to simultaneously assess cell viability and reporter activity, as well as for flow-cytometry-based applications. In sum, we established reporter NiVs that will not only facilitate antiviral screening, but also the study of cellular components that influence viral replication.

Acknowledgments

We thank Mike Flint for helpful discussions and suggestions. The findings and conclusions in this report are those of the authors and do not necessarily represent those of the Centers for Disease Control and Prevention.

References

Aljofan M, Porotto M, Moscona A, Mungall BA. Development and validation of a chemiluminescent immunodetection assay amenable to high throughput screening of antiviral drugs for Nipah and Hendra virus. J Virol Methods. 2008; 149:12–19. [PubMed: 18313148]

Bono VH Jr, Weissman SM, Frei E 3rd. The effect of 6-azauridine administration on De Novo pyrimidine production in chronic myelogenous leukemia. J Clin Investig. 1964; 43:1486–1494. [PubMed: 14192530]

Bossart KN, Mungall BA, Crameri G, Wang LF, Eaton BT, Broder CC. Inhibition of Henipavirus fusion and infection by heptad-derived peptides of the Nipah virus fusion glycoprotein. Virol J. 2005; 2:57. [PubMed: 16026621]

Broder CC, Xu K, Nikolov DB, Zhu Z, Dimitrov DS, Middleton D, Pallister J, Geisbert TW, Bossart KN, Wang LF. A treatment for and vaccine against the deadly Hendra and Nipah viruses. Antiviral Res. 2013; 100:8–13. [PubMed: 23838047]

Buchholz UJ, Finke S, Conzelmann KK. Generation of bovine respiratory syncytial virus (BRSV) from cDNA: BRSV NS2 is not essential for virus replication in tissue culture, and the human RSV leader region acts as a functional BRSV genome promoter. J Virol. 1999; 73:251–259. [PubMed: 9847328]

Chiang CF, Lo MK, Rota PA, Spiropoulou CF, Rollin PE. Use of monoclonal antibodies against Hendra and Nipah viruses in an antigen capture ELISA. Virol J. 2010; 7:115. [PubMed: 20525276]

Corish P, Tyler-Smith C. Attenuation of green fluorescent protein half-life in mammalian cells. Protein Eng. 1999; 12:1035–1040. [PubMed: 10611396]

Dhondt KP, Mathieu C, Chalons M, Reynaud JM, Vallve A, Raoul H, Horvat B. Type I interferon signaling protects mice from lethal henipavirus infection. J Infect Dis. 2013; 207:142–151. [PubMed: 23089589]

Escaffre O, Borisevich V, Carmical JR, Prusak D, Prescott J, Feldmann H, Rockx B. Henipavirus pathogenesis in human respiratory epithelial cells. J Virol. 2013; 87:3284–3294. [PubMed: 23302882]

Freiberg A, Dolores LK, Enterlein S, Flick R. Establishment and characterization of plasmid-driven minigenome rescue systems for Nipah virus: RNA polymerase I- and T7-catalyzed generation of functional paramyxoviral RNA. Virology. 2008; 370:33–44. [PubMed: 17904180]

Georges-Courbot MC, Contamin H, Faure C, Loth P, Baize S, Leyssen P, Neyts J, Deubel V. Poly(I)-poly(C12U) but not ribavirin prevents death in a hamster model of Nipah virus infection. Antimicrob Agents Chemother. 2006; 50:1768–1772. [PubMed: 16641448]

Gutowski GE, Sweeney MJ, DeLong DC, Hamill RL, Gerzon K, Dyke RW. Biochemistry and biological effects of the pyrazofurins (pyrazomycins): initial clinical trial. Ann N Y Acad Sci. 1975; 255:544–551. [PubMed: 1059372]

Kim JH, Lee SR, Li LH, Park HJ, Park JH, Lee KY, Kim MK, Shin BA, Choi SY. High cleavage efficiency of a 2A peptide derived from porcine teschovirus-1 in human cell lines, zebrafish and mice. PLoS ONE. 2011; 6:e18556. [PubMed: 21602908]

Kolakofsky D, Pelet T, Garcin D, Hausmann S, Curran J, Roux L. Paramyxovirus RNA synthesis and the requirement for hexamer genome length: the rule of six revisited. J Virol. 1998; 72:891–899. [PubMed: 9444980]

Kulkarni S, Volchkova V, Basler CF, Palese P, Volchkov VE, Shaw ML. Nipah virus edits its P gene at high frequency to express the V and W proteins. J Virol. 2009; 83:3982–3987. [PubMed: 19211754]

Lo MK, Peeples ME, Bellini WJ, Nichol ST, Rota PA, Spiropoulou CF. Distinct and overlapping roles of Nipah virus P gene products in modulating the human endothelial cell antiviral response. PLoS ONE. 2012; 7:e47790. [PubMed: 23094089]

Loening AM, Fenn TD, Wu AM, Gambhir SS. Consensus guided mutagenesis of Renilla luciferase yields enhanced stability and light output. Protein Eng Des Sel. 2006; 19:391–400. [PubMed: 16857694]

Luby SP. The pandemic potential of Nipah virus. Antiviral Res. 2013; 100:38–43. [PubMed: 23911335]

Marsh GA, Virtue ER, Smith I, Todd S, Arkinstall R, Frazer L, Monaghan P, Smith GA, Broder CC, Middleton D, Wang LF. Recombinant Hendra viruses expressing a reporter gene retain pathogenicity in ferrets. Virol J. 2013; 10:95. [PubMed: 23521919]

Nahar N, Mondal UK, Sultana R, Hossain MJ, Khan MS, Gurley ES, Oliveras E, Luby SP. Piloting the use of indigenous methods to prevent Nipah virus infection by interrupting bats' access to date palm sap in Bangladesh. Health Promot Int. 2013; 28:378–386. [PubMed: 22669914]

Porotto M, Orefice G, Yokoyama CC, Mungall BA, Realubit R, Sganga ML, Aljofan M, Whitt M, Glickman F, Moscona A. Simulating henipavirus multicycle replication in a screening assay leads to identification of a promising candidate for therapy. J Virol. 2009; 83:5148–5155. [PubMed: 19264786]

Rodriguez JJ, Parisien JP, Horvath CM. Nipah virus V protein evades alpha and gamma interferons by preventing STAT1 and STAT2 activation and nuclear accumulation. J Virol. 2002; 76:11476–11483. [PubMed: 12388709]

Rota PA, Lo MK. Molecular virology of the henipaviruses. Curr Top Microbiol Immunol. 2012; 359:41–58. [PubMed: 22552699]

Shaw ML, Cardenas WB, Zamarin D, Palese P, Basler CF. Nuclear localization of the Nipah virusWprotein allows for inhibition of both virus- and toll-like receptor 3-triggered signaling pathways. J Virol. 2005; 79:6078–6088. [PubMed: 15857993]

Talekar A, Pessi A, Glickman F, Sengupta U, Briese T, Whitt MA, Mathieu C, Horvat B, Moscona A, Porotto M. Rapid screening for entry inhibitors of highly pathogenic viruses under low-level biocontainment. PLoS ONE. 2012; 7:e30538. [PubMed: 22396728]

Tamin A, Harcourt BH, Lo MK, Roth JA, Wolf MC, Lee B, Weingartl H, Audonnet JC, Bellini WJ, Rota PA. Development of a neutralization assay for Nipah virus using pseudotype particles. J Virol Methods. 2009; 160:1–6. [PubMed: 19559943]

Virtue ER, Marsh GA, Wang LF. Interferon signaling remains functional during henipavirus infection of human cell lines. J Virol. 2011; 85:4031–4034. [PubMed: 21289115]

Wang YE, Park A, Lake M, Pentecost M, Torres B, Yun TE, Wolf MC, Holbrook MR, Freiberg AN, Lee B. Ubiquitin-regulated nuclearcytoplasmic trafficking of the Nipah virus matrix protein is important for viral budding. PLoS Pathog. 2010; 6:e1001186. [PubMed: 21085610]

Yan D, Krumm SA, Sun A, Steinhauer DA, Luo M, Moore ML, Plemper RK. Dual myxovirus screen identifies a small-molecule agonist of the host antiviral response. J Virol. 2013; 87:11076–11087. [PubMed: 23926334]

Yoneda M, Guillaume V, Ikeda F, Sakuma Y, Sato H, Wild TF, Kai C. Establishment of a Nipah virus rescue system. Proc Nat Acad Sci USA. 2006; 103:16508–16513. [PubMed: 17053073]

Zhang JH, Chung TD, Oldenburg KR. A simple statistical parameter for use in evaluation and validation of high throughput screening assays. J Biomol Screen. 1999; 4:67–73. [PubMed: 10838414]

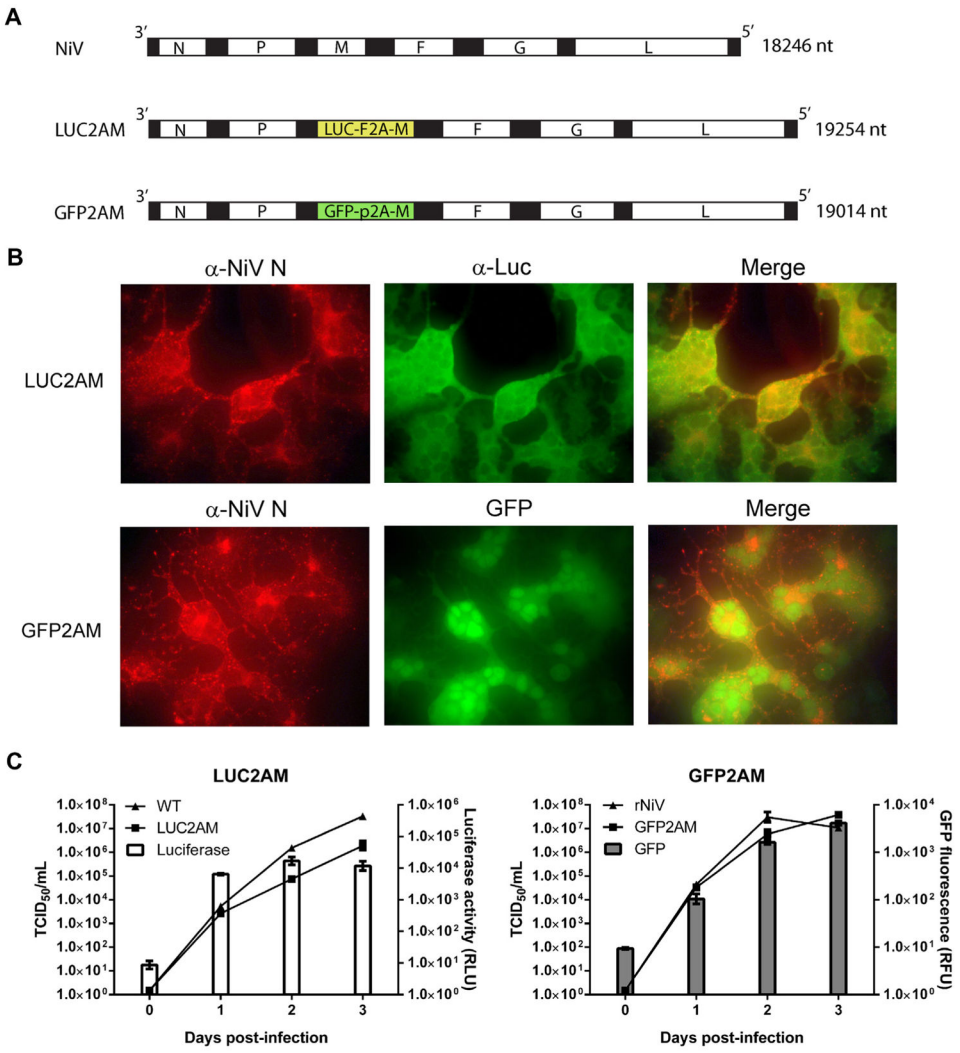

Fig. 1.

Design and characterization of reporter Nipah (NiV) viruses. (A) Schematic of wild-type NiV genome alongside reporter NiVs expressing either luciferase (LUC2AM) or green-fluorescent protein (GFP2AM) respective nucleotide (nt) lengths indicated. Black segments represent non-coding regions, while white segments indicate open reading frames. Modified M gene coding regions for LUC2AM and GFP2AM are highlighted in yellow and green respectively. (B) Microscopic examination of HeLa cells infected with LUC2AM and GFP2AM. LUC2AM-infected were stained with antibodies against NiV nucleoprotein (N) and anti-Renilla luciferase antibodies, while GFP2AM-infected cells were stained only with N antibodies. (C) Time course analysis of growth kinetics and reporter activities of LUC2AM and GFP2AM alongside the growth kinetics of their corresponding wild-type recombinant NiVs (WT, rNiV respectively). Vero cells were infected with each virus at an MOI of 0.01. At 1, 2, and 3 days post-infection, supernatants titers were determined by $TCID_{50}$, (left *Y*-axis) while relative light units (RLU) or relative fluorescence units (RFU) in the cells infected with reporter viruses were measured (right *Y*-axis). Reporter activity levels

at day 0 post-infection indicate background noise of the luminometer/fluorometer. Values represent means and standard deviations for 3 experiments.

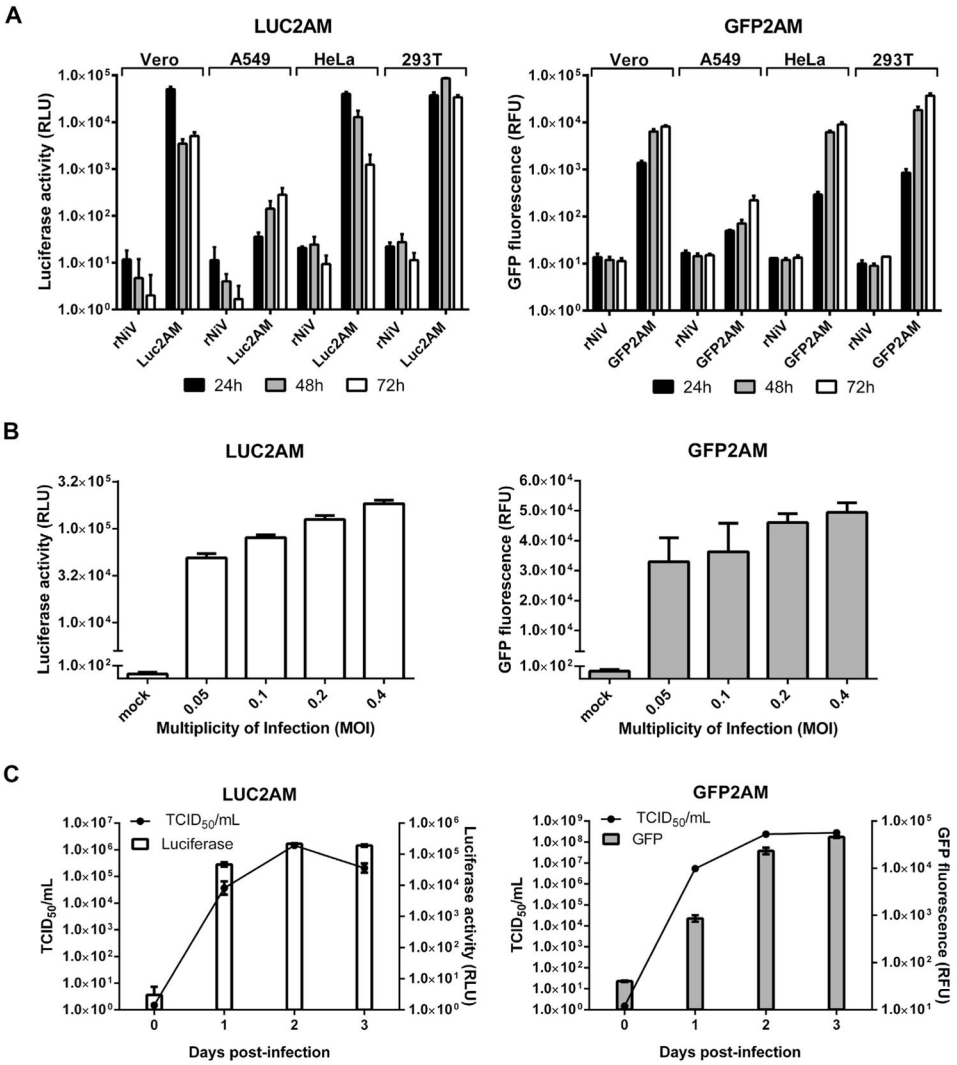

Fig. 2.

Assay optimization. (A) 293T cells yielded the highest reporter activity levels for both LUC2AM and GFP2AM reporter viruses. (B) 293T cells were infected at the indicated multiplicity of infection (MOI) with LUC2AM or GFP2AM, and respective reporter values were measured at 48 hpi. (C) Time course analysis of growth kinetics and reporter activities of LUC2AM and GFP2AM in 293T cells (MOI = 0.2 $TCID_{50}$/cell). At 1, 2, and 3 days post-infection, supernatant titers were determined by $TCID_{50}$ (left *Y*-axis), while respective reporter activities in the cells were measured (right *Y*-axis). Values represent means and standard deviations for 3 experiments.

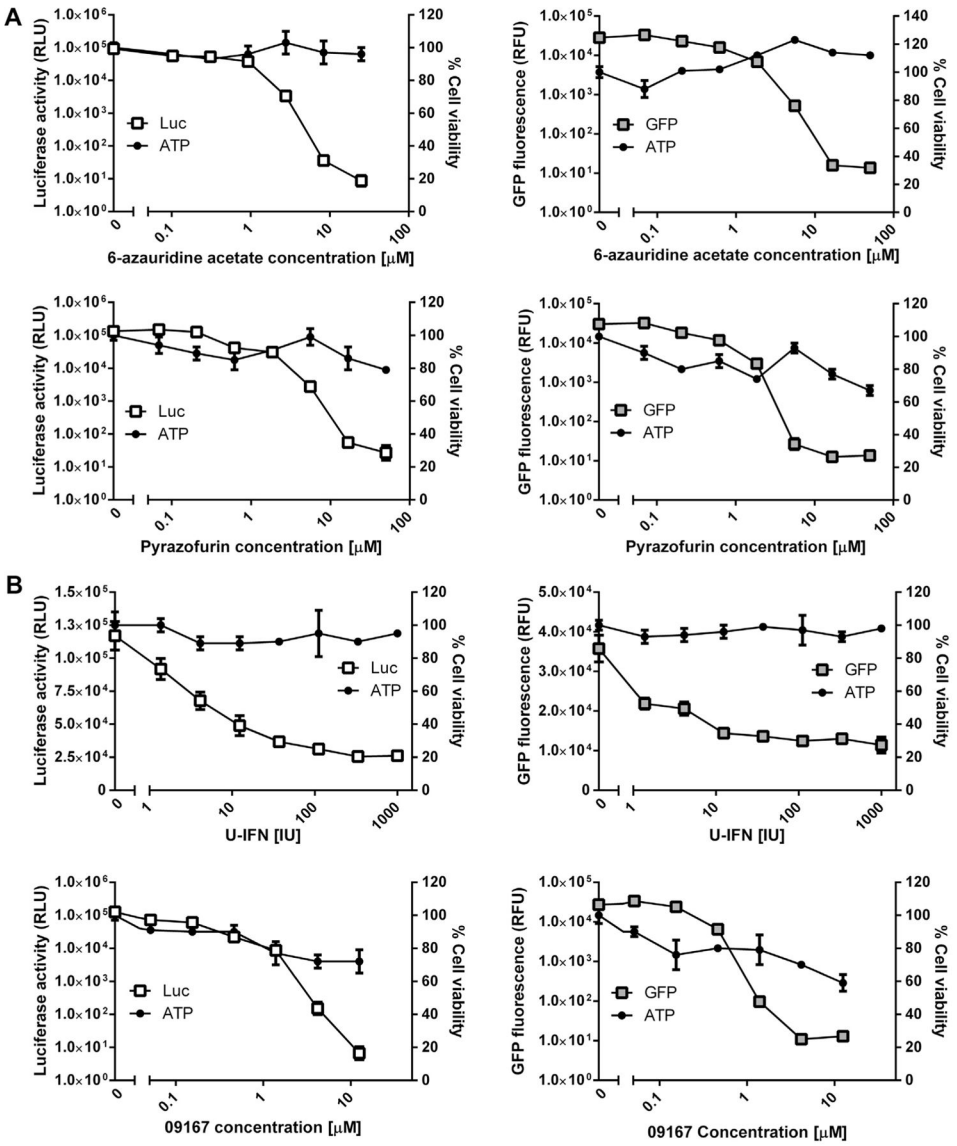

Fig. 3.

Reporter NiVs as tools for antiviral testing. (A) Testing of 2 known inhibitors (6-azauridine acetate and pyrazofurin) of pyrimidine biosynthesis and (B) 2 innate immune agonists (Universal interferon and compound 09167) against LUC2AM (left panels) and GFP2AM (right panels). 293T cells were infected with reporter NiVs (MOI = 0.2 $TCID_{50}$/cell) for 2 h, and then incubated with indicated compounds in 3-fold serial dilutions. Each concentration was assessed in three replicates. Reporter virus activity was measured on the left *Y*-axis; % cell viability was measured on the right *Y*-axis. Values represent means and standard deviations of 3 experiments.

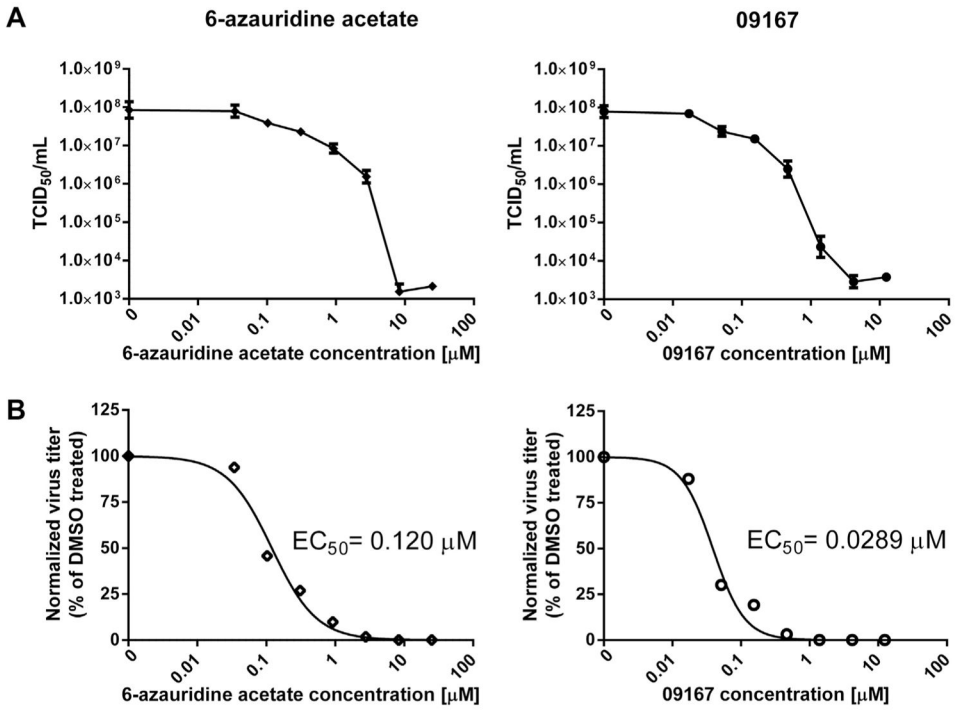

Fig. 4.

Confirmatory counter-screening against wild-type NiV. (A) Virus titer-reduction assays. 293T cells were infected with wild-type NiV (MOI = 0.2 $TCID_{50}$/cell) for 2 h, and then incubated with 3-fold dilutions of 6-azauridine acetate (left panel) or compound 09167 (right panel) for 48 h. Supernatant virus titers were determined by $TCID_{50}$ titrations and plotted against compound concentration. Values represent means and standard deviations of 3 experiments. Virus titers were then (B) normalized to vehicle (DMSO) controls. EC_{50}s were calculated based on four-parameter variable-slope nonlinear regression models. Normalized data points represent means for three experiments.

Table 1

50% effective concentrations (EC_{50}) of compounds against reporter and wild-type NiVs (therapeutic indices in parentheses).

Inhibitor ID	Units	NiV-LUC2AM	NiV-GFP2AM	NiV-MY-99
6-Azauridine acetate	μM	0.274 ± 0.0357 (⩾364)	0.553 ± 0.151 (⩾180)	0.120 ± 0.0445 (⩾833)
Pyrazofurin	μM	0.432 ± 0.0871 (⩾115)	0.281 ± 0.0448 (⩾177)	ND
09167	μM	0.0723 ± 0.0123 (877)	0.254 ± 0.0905 (249)	0.0289 ± 0.0102 (2196)
U-IFN	IU	10.96 ± 4.90 (⩾91)	10.2 ± 8.49 (⩾98)	ND

ND - Not done.

Table 2

Comparison of Nipah LUC2AM and GFP2AM assays used in this study.

Plate format	Target virus[a]	Z′value[b]	S/N ratio[c]	%CV
96 wells	NiV-LUC2AM	0.85	1.33E + 04	5%
96 wells	NiV-GFP2AM	0.67	2.16E + 03	11%

[a] 293T cells were infected with either LUC2AM or GFP2AM viruses for 2 h before treatment with host antiviral agonist compound 09167 (final concentration, 12.5 mM) or an equivalent amount of vehicle (DMSO). Relative luciferase/fluorescence units were determined at 48 hpi.

[b] Z' factor (Zhang et al., 1999). Statistical analyses were based on means of four independent experiments.

[c] Ratio of signal to background noise.